

Modelling the excavation damaged zone in Callovo-Oxfordian claystone using shear strain localisation

B. Pardoen - F. Collin



Excavation damaged zone

Long-term management of radioactive wastes



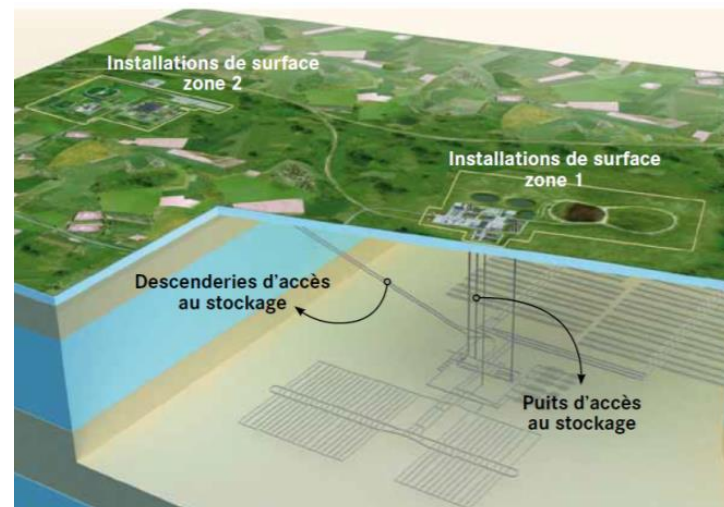
Intermediate
(long-lived)
&
high activity
wastes



Deep geological disposal

Repository in deep
geological media with
good confining properties
(Low permeability
 $K<10^{-12} \text{ m/s}$)

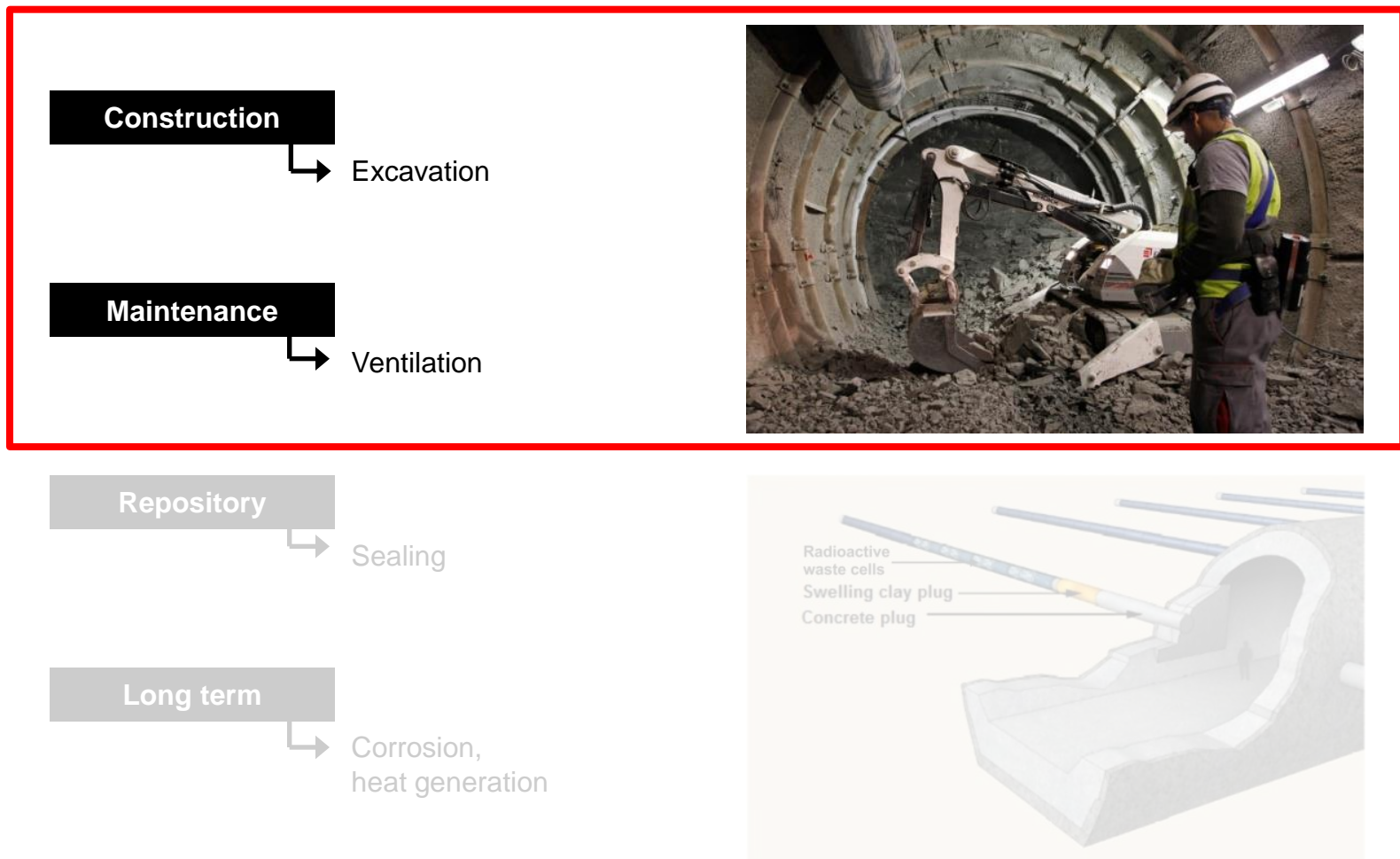
Underground structures
= network of galleries



Disposal facility of Cigéo project in France
(Labalette et al., 2013)

Excavation damaged zone

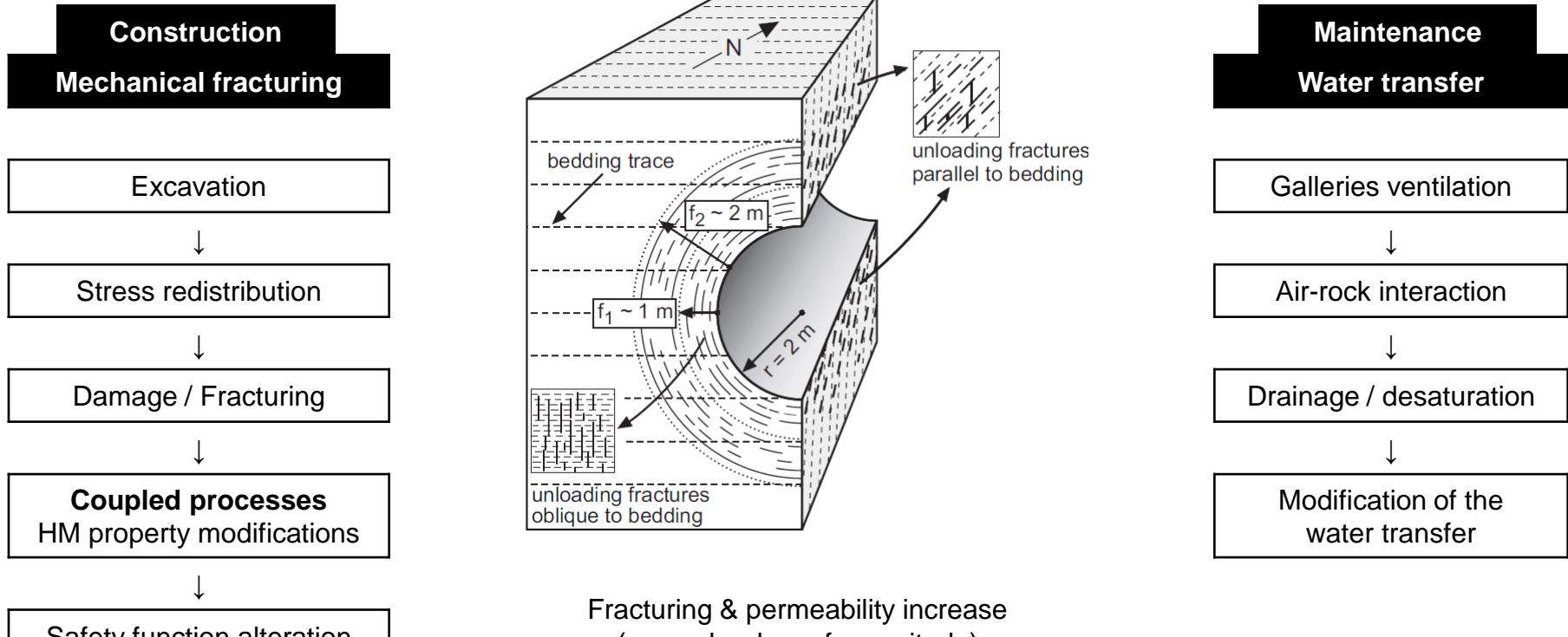
Repository phases



Type C wastes (Andra, 2005)

Excavation damaged zone

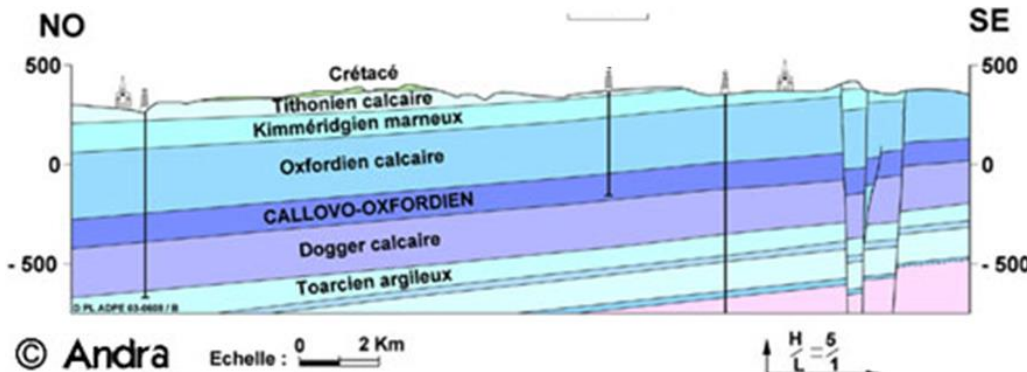
Excavation Damaged Zone (EDZ)



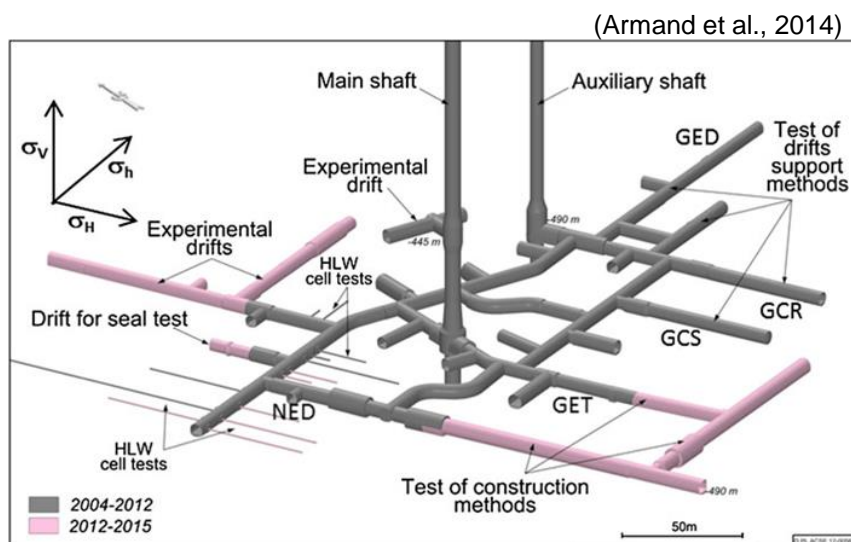
Excavation damaged zone

Callovo-Oxfordian claystone (COx)

Sedimentary clay rock (France).



- Underground research laboratory
- Feasibility of a safe repository
- France (Meuse / Haute-Marne, Bure)

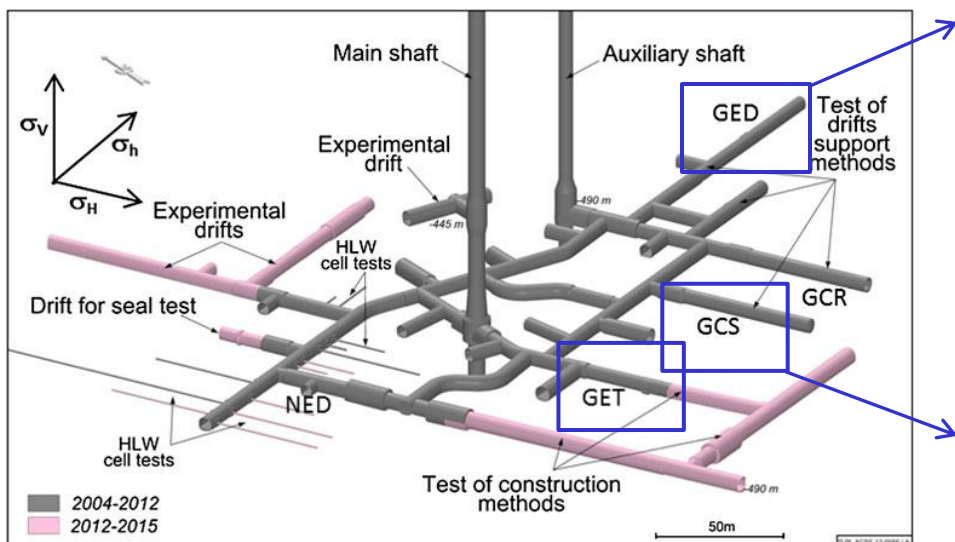


Excavation damaged zone

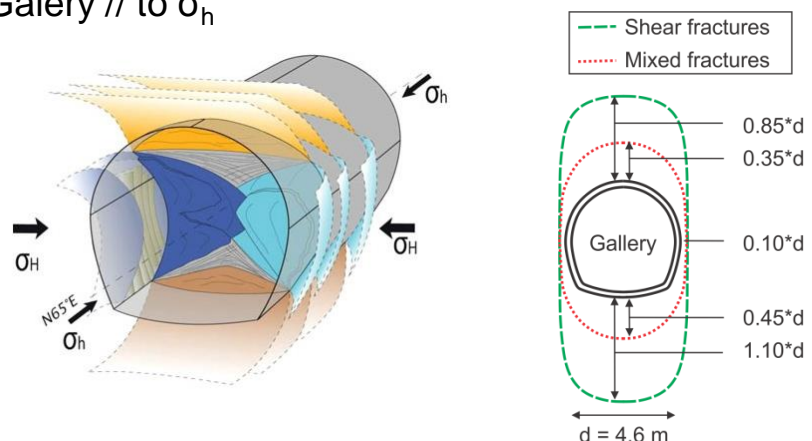
In situ evidences (Andra) :

(Armand et al. 2014)

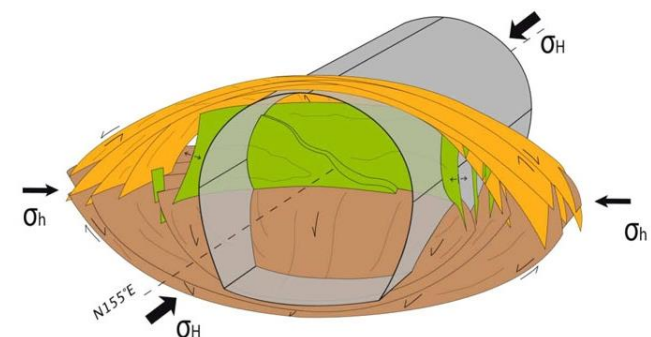
- Anisotropy: - stress : $\sigma_H > \sigma_h \sim \sigma_v$
- material : cross-anisotropy



Galery // to σ_h



Galery // to σ_H



Major issues : prediction of the extension, fracturing structure and properties modifications.

Study :
- fractures modelling with shear strain localisation
- influence of permeability variation

Outline

1. CONSTITUTIVE MODELS

2. FRACTURES MODELLING

- GALLERY // TO σ_h
- GALLERY // TO σ_H

3. PERMEABILITY EVOLUTION

1. Constitutive models

1.1 Strain localisation with regularization - Coupled 2^d gradient model : (Chambon et al., 1998 and 2001)

The continuum is enriched with microstructure effects. The kinematics include the classical one (macro) and the microkinematics (Toupin 1962, Mindlin 1964, Germain 1973).

Biphasic porous media : solid + fluid (Collin et al., 2006)

Balance equations for biphasic porous media :

$$\int_{\Omega} \left(\sigma_{ij} \frac{\partial u_i^*}{\partial x_j} + \Sigma_{ijk} \frac{\partial^2 u_i^*}{\partial x_j \partial x_k} \right) d\Omega = \int_{\Omega} G_i u_i^* d\Omega + \int_{\Gamma_\sigma} \left(\bar{t}_i u_i^* + \bar{T}_i D u_i^* \right) d\Gamma$$

$$\int_{\Omega} \left(\frac{\partial M}{\partial t} p_w^* - m_{w,i} \frac{\partial p_w^*}{\partial x_i} \right) d\Omega = \int_{\Omega} Q p_w^* d\Omega + \int_{\Gamma_q} \bar{q} p_w^* d\Gamma$$

Bishop's effective stress :

$$\sigma_{ij} = \sigma'_{ij} - b_{ij} S_{rw} p_w \delta_{ij}$$

Double stress : $\tilde{\Sigma}_{ijk} = f \left(B, \frac{\partial^2 u_i^*}{\partial x_j \partial x_k} \right)$

1. Constitutive models

1.2 Mechanical model :

Linear elasticity : Cross-anisotropic (5 param.) + Biot's coefficient

$$d\varepsilon_{ij}^e = D_{ijkl}^e d\sigma_{kl}$$

$$E_{//}, E_{\perp}, \nu_{///}, \nu_{//\perp}, G_{//\perp}$$

$$b_{ij} = \delta_{ij} - \frac{C_{ijk}^e}{3K_s}$$

$$b_{ij} = \begin{bmatrix} b_{//} & & \\ & b_{//} & \\ & & b_{\perp} \end{bmatrix}$$

$$\frac{\nu_{\perp//}}{E_{\perp}} = \frac{\nu_{//\perp}}{E_{//}}$$

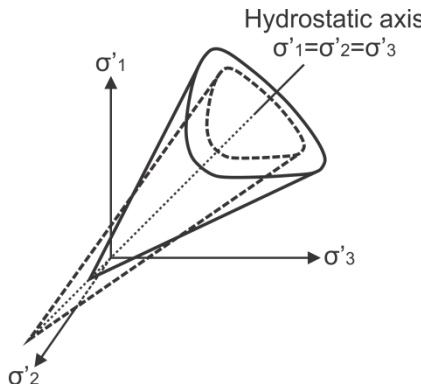
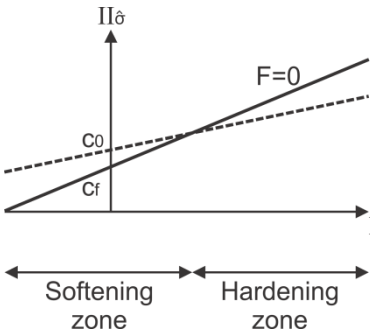
$$D_{ijkl}^e = \begin{bmatrix} \frac{1}{E_{//}} & -\frac{\nu_{///}}{E_{//}} & -\frac{\nu_{\perp//}}{E_{\perp}} & & \\ -\frac{\nu_{///}}{E_{//}} & \frac{1}{E_{//}} & -\frac{\nu_{\perp//}}{E_{\perp}} & & \\ -\frac{\nu_{\perp//}}{E_{\perp}} & -\frac{\nu_{//\perp}}{E_{//}} & \frac{1}{E_{\perp}} & & \\ & & & \frac{1+\nu_{///}}{E_{//}} & \\ & & & & \frac{1}{2G_{//\perp}} \\ & & & & \frac{1}{2G_{//\perp}} \end{bmatrix}$$

Plasticity :

Van Eeckelen yield surface

Hardening/softening of ϕ/c :

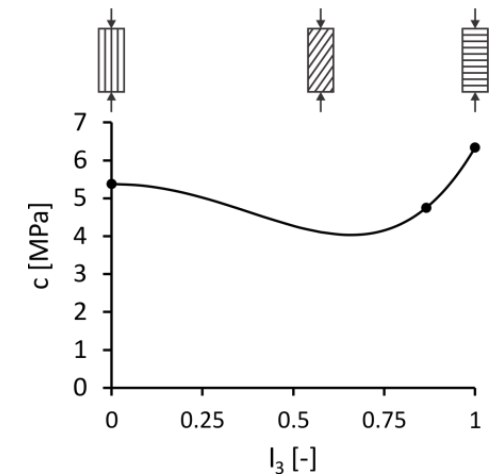
$$F \equiv II_{\hat{\sigma}} - m \left(I_{\sigma'} + \frac{3c}{\tan \phi_c} \right) = 0$$



Cohesion anisotropy :

$$c = a_{ij} l_i l_j = \bar{c} \left(1 + A_{11}(1 - 3l_3^2) + b_1 A_{11}^2 (1 - 3l_3^2)^2 + \dots \right)$$

$$l_i = \sqrt{\frac{\sigma_{i1}'^2 + \sigma_{i2}'^2 + \sigma_{i3}'^2}{\sigma_{ij}' \sigma_{ij}'}}$$



1. Constitutive models

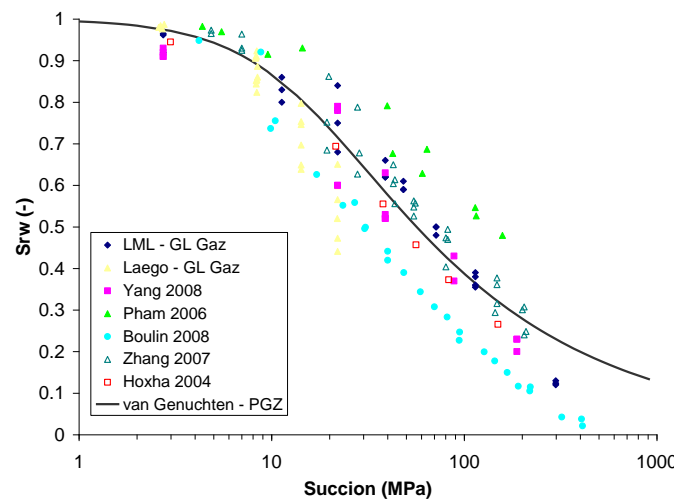
1.3 Flow model :

Advection of liquid phase (Darcy's flow) :

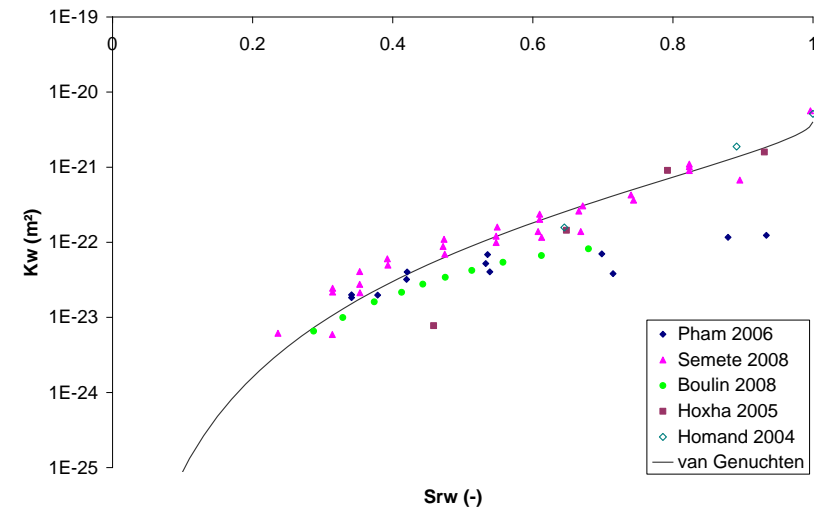
$$m_{w,i} = -\rho_w \frac{k_{ij} k_{r,w}}{\mu_w} \frac{\partial p_w}{\partial x_j}$$

Water retention and permeability curves (Van Genuchten's model) :

$$S_{r,w} = S_{res} + (S_{max} - S_{res}) \left[1 + \left(\frac{P_c}{P_r} \right)^n \right]^{-m}$$



$$k_{r,w} = \sqrt{S_{r,w}} \left[1 - \left(1 - S_{r,w}^{1/m} \right)^m \right]^2$$



2. Fractures modelling

2.1 Gallery // to σ_h :

Anisotropic stress state, isotropic model

HM modelling in 2D plane strain state (LAGAMINE-Ulg) :

Anisotropy (Andra URL) :

→ hydraulic permeability anisotropy

$$k_{\text{hor/vert}} = 4 \cdot 10^{-20} / 1.33 \cdot 10^{-20} [\text{m}^2]$$

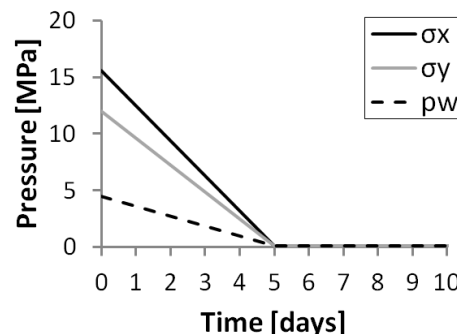
→ initial anisotropic stress state

$$p_{w,0} = 4.5 [\text{MPa}]$$

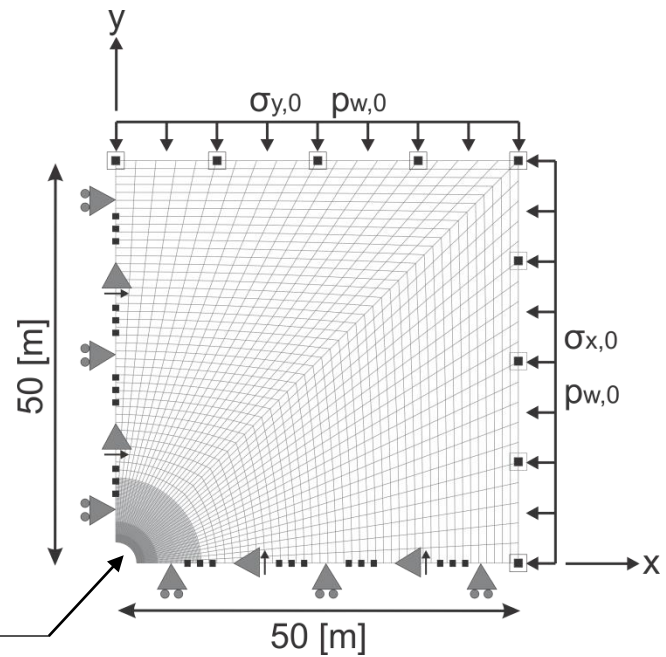
$$\sigma_{v,0} = \sigma_{h,0} = 12 [\text{MPa}]$$

$$\sigma_{H,0} = 1.3 \sigma_{v,0} = 15.6 [\text{MPa}]$$

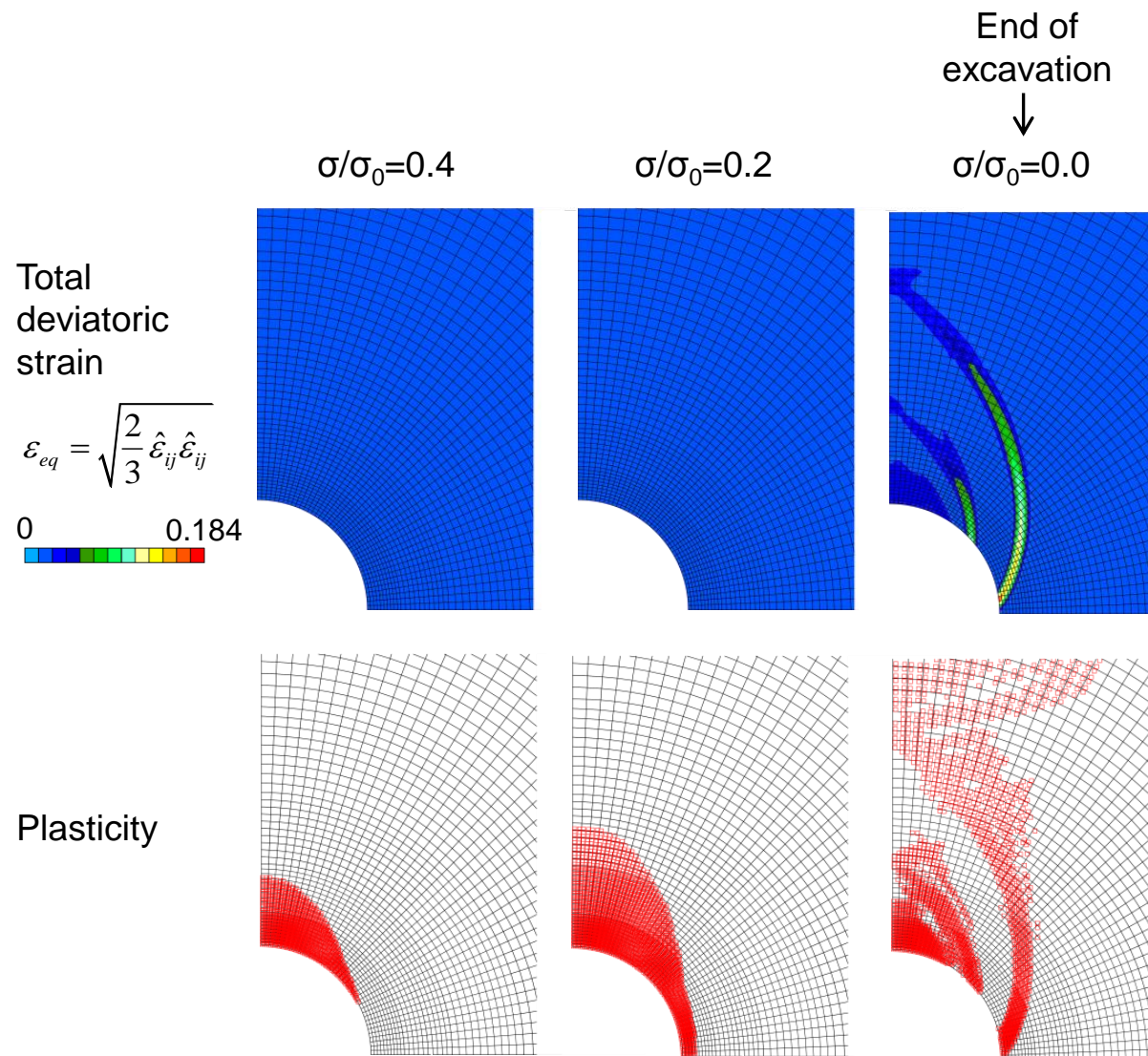
Excavation :



- Constant pore water pressure ($p_{w,0}$)
- ← Constant total stress ($\sigma_{y,0} / \sigma_{x,0}$)
- Constrained displacement perpendicular to the boundary
- ▲ Constrained normal derivative of the radial displacement
- Impervious boundary

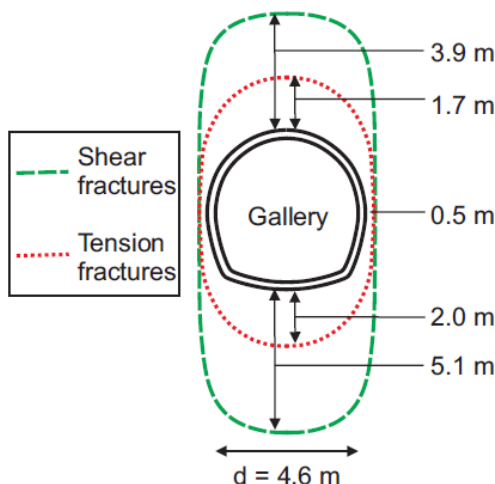


2. Fractures modelling

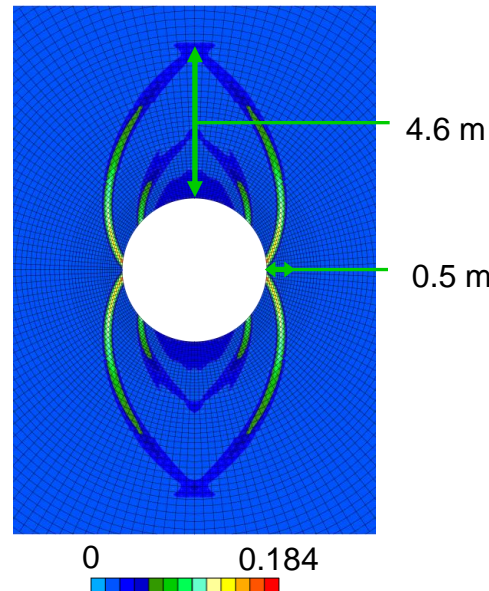


2. Fractures modelling

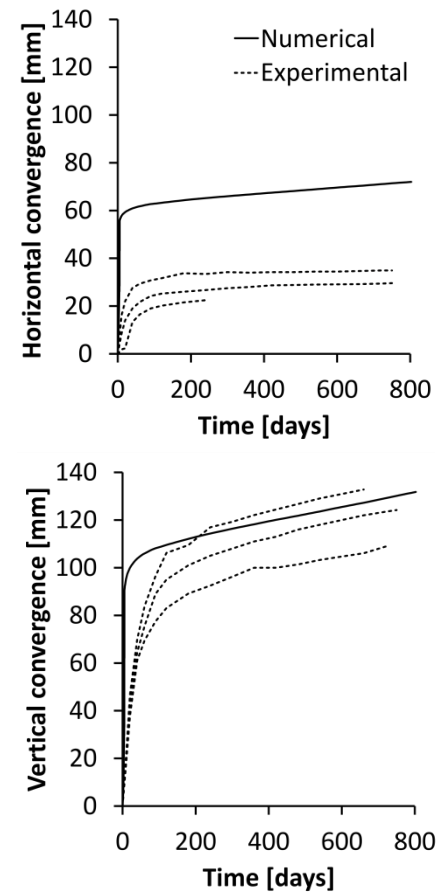
Fractures



Total deviatoric strain



Convergence



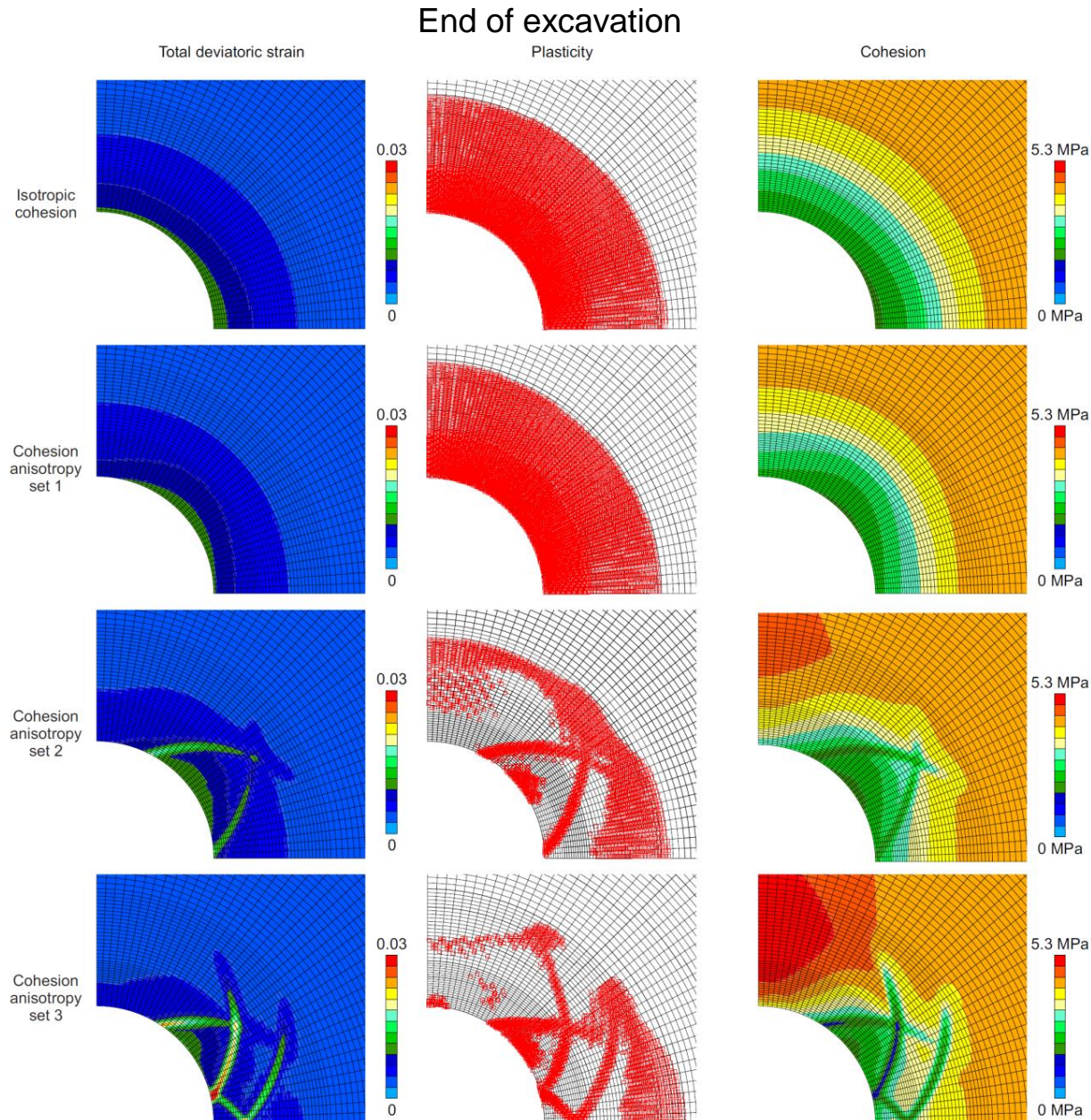
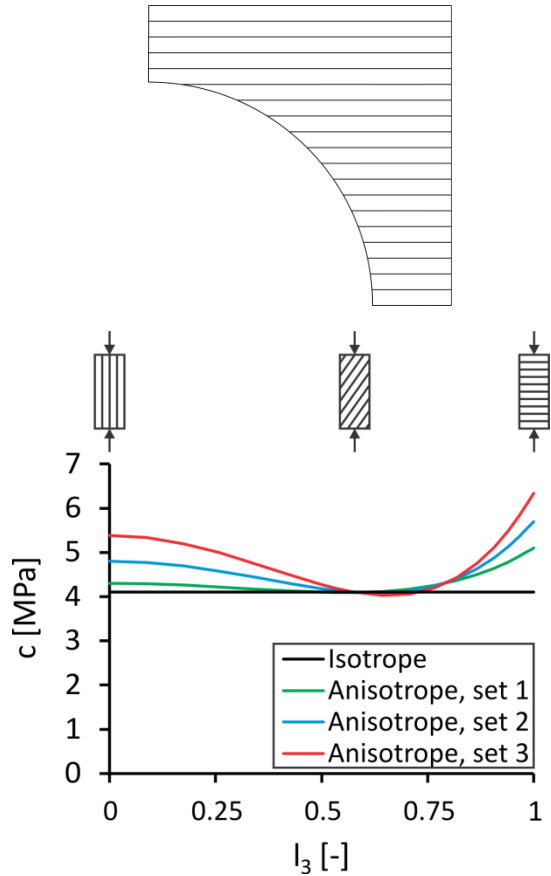
σ anisotropy is the predominant factor leading to strain localisation and to the elliptical shape of the damaged zone.

2. Fractures modelling

2.2 Gallery // to σ_H :

Isotropic stress state ($\sigma=12$ MPa),
anisotropic model

HM modelling in 2D plane
strain state



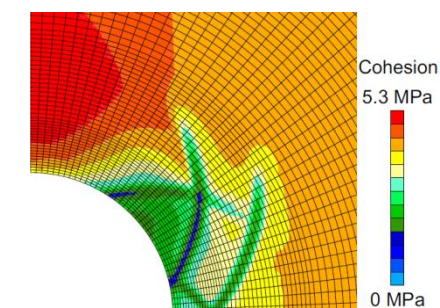
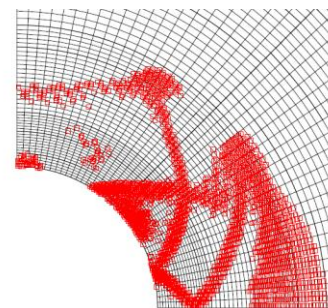
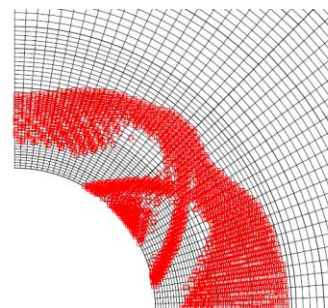
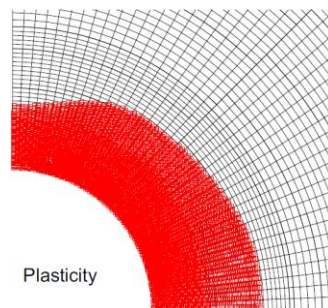
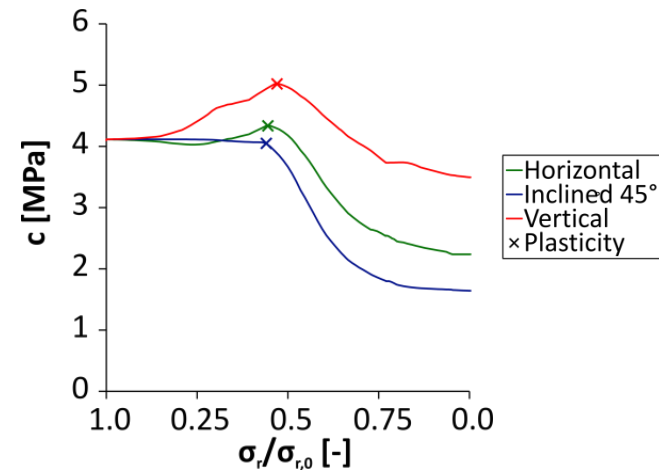
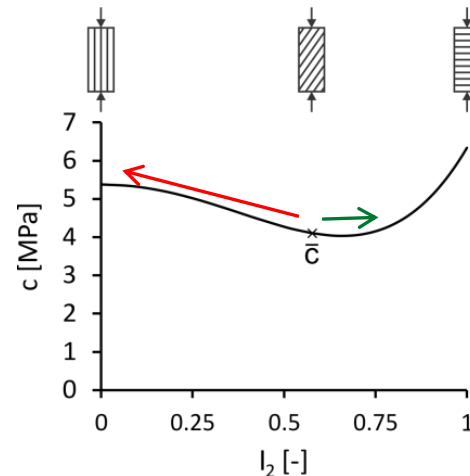
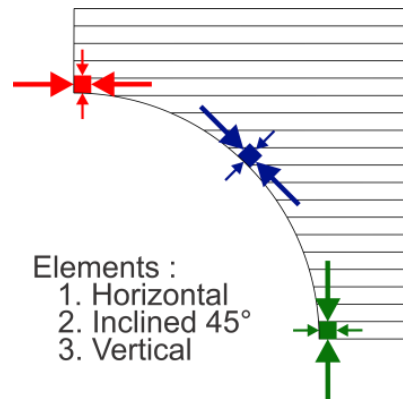
2. Fractures modelling

Cohesion evolution :

Anisotropy: $c = a_{ij}l_il_j = \bar{c} \left(1 + A_{11}(1 - 3l_2^2) + b_1 A_{11}^2 (1 - 3l_2^2)^2 + \dots \right)$ $l_i = \sqrt{\frac{\sigma_{i1}^2 + \sigma_{i2}^2 + \sigma_{i3}^2}{\sigma_{ij}\sigma_{ij}}}$

Initially : isotropic $\sigma_{ij} \rightarrow c = \bar{c}$ $l_2 = \sqrt{3}/3 = 0.58$

Excavation : $\sigma_r \downarrow$ and $\sigma_{ort} \uparrow$

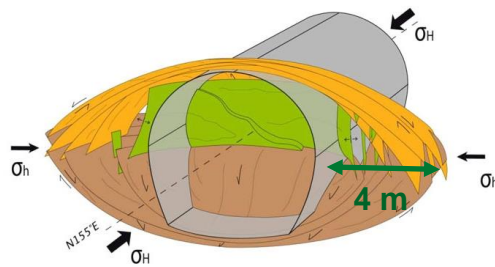


2. Fractures modelling

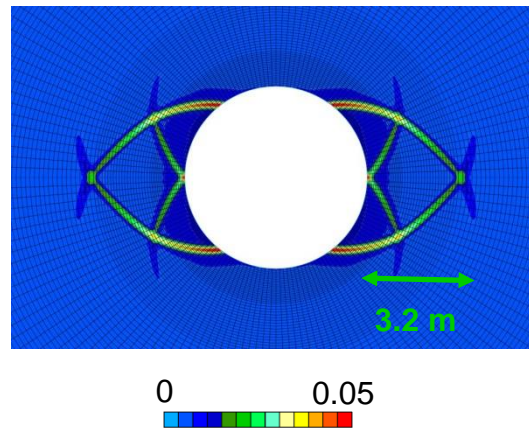
Anisotropic stress state, anisotropic model

$$\sigma_{H,0} = 1.3 \sigma_{v,0} > \sigma_{v,0} = \sigma_{h,0} = 12 \text{ [MPa]}$$

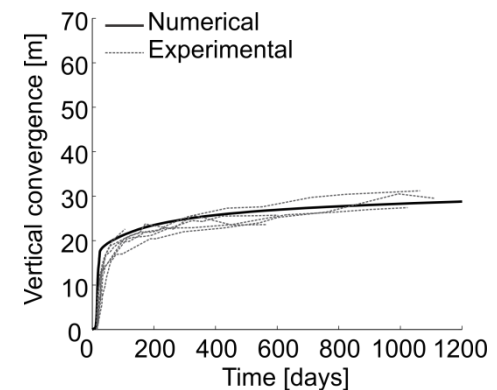
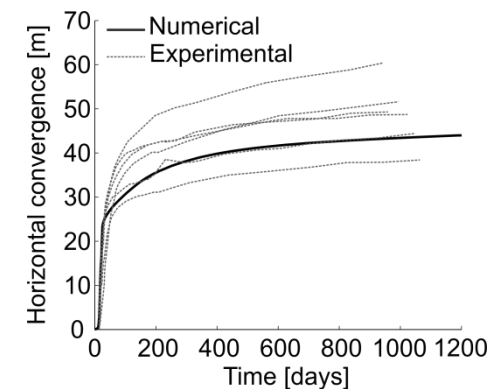
Fractures



Total deviatoric strain



Convergence



Isotropic stress state in the gallery section does not lead to shear strain localisation unless the material anisotropy is considered.

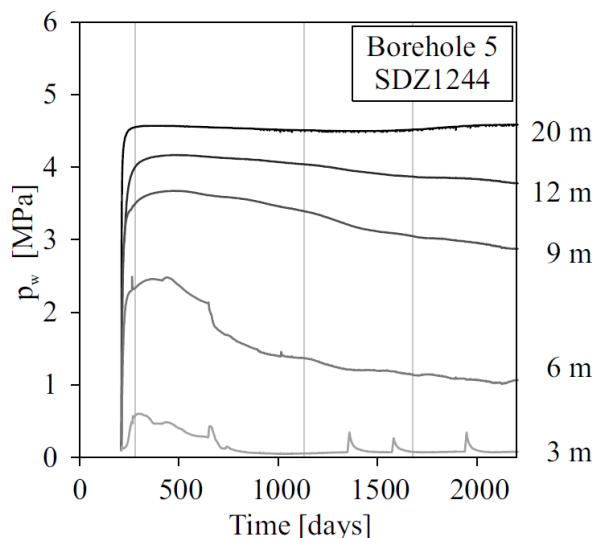
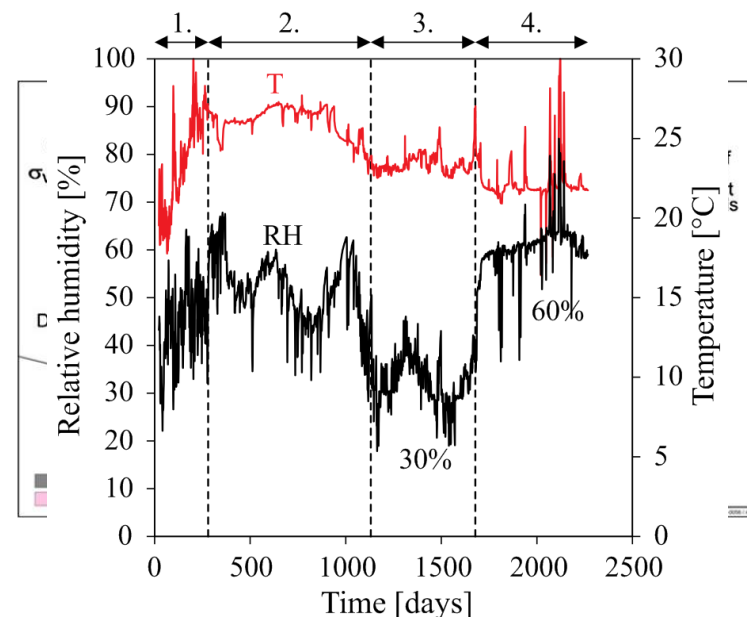
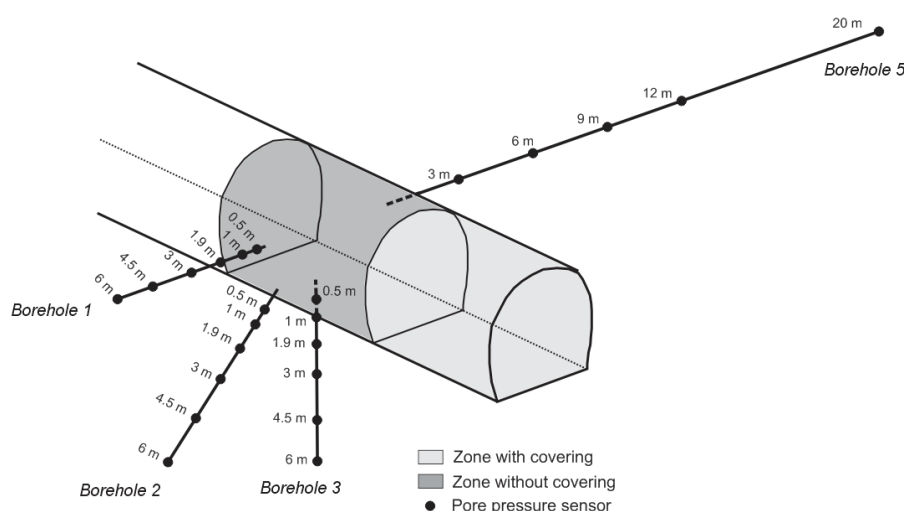
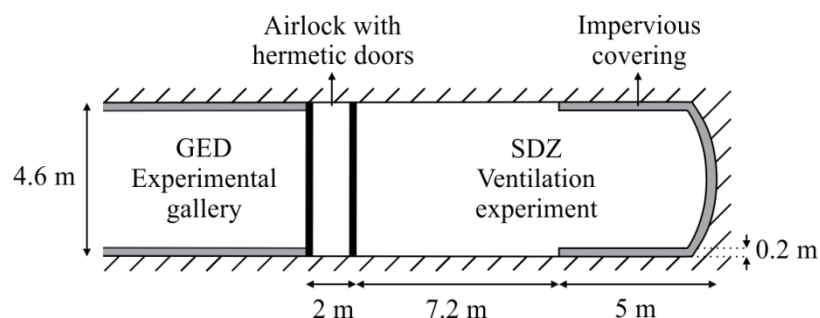
Material anisotropy seems to be the predominant factor leading to strain localisation and to the elliptical shape of the damaged zone.

3. Permeability evolution

3.1 Large-scale experiment of gallery ventilation (SDZ)

Characterise the effect of gallery ventilation on the hydraulic transfer around it.

- drainage / desaturation
- exchange at gallery wall

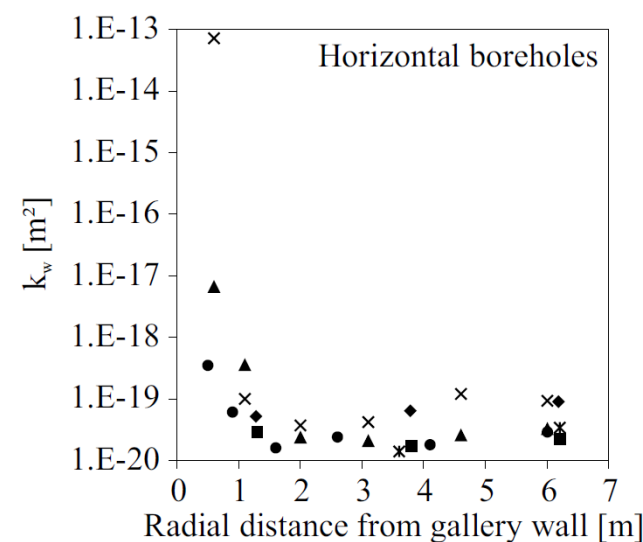
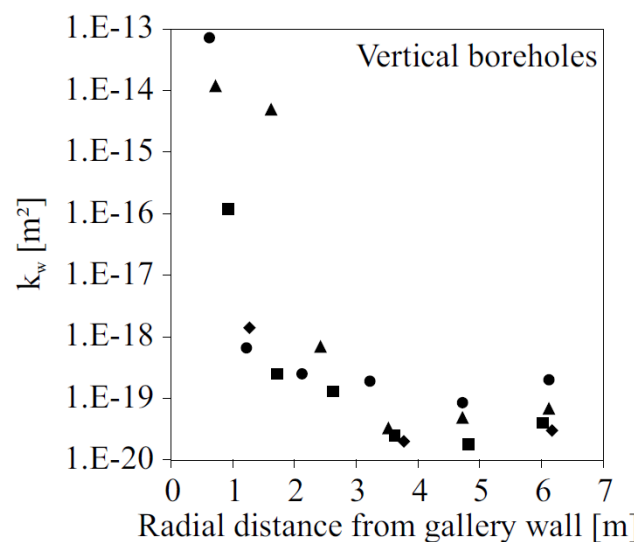
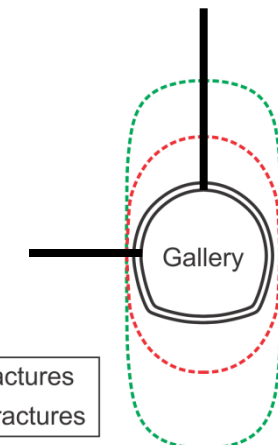


3. Permeability evolution

Permeability variation in fractured zone

HM coupling in the EDZ.

Saturated permeability in boreholes



Fracture and rock matrix permeabilities

- Capture k_w evolution
- Relation to fractures

3. Permeability evolution

Evolution of intrinsic water permeability

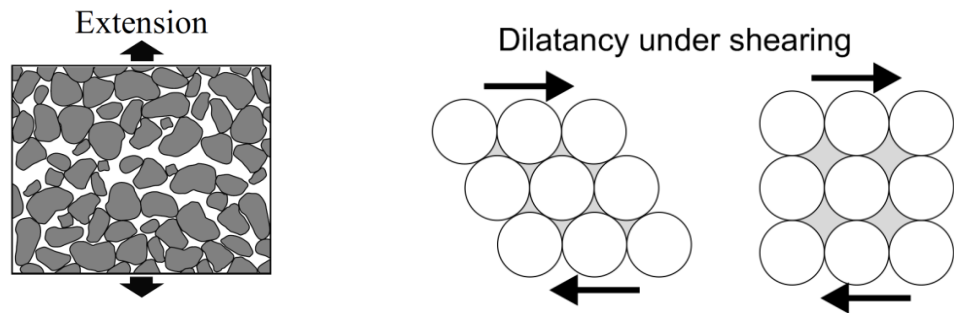
Various approaches: deformation, damage, cracks...

- Relation to deformation

Volumetric effects = increase of porous space
(Kozeny-Carman)

$$k_w = k_{w,0} \frac{(1-\phi_0)^{\xi_1}}{\phi_0^{\xi_2}} \frac{\phi^{\xi_2}}{(1-\phi)^{\xi_1}}$$

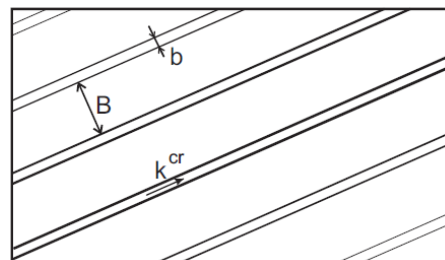
$$\varepsilon_v = \frac{\varepsilon_{ii}}{3}$$



- Fracture permeability

Cubic law for parallel-plate approach
(Witherspoon 1980; Snow 1969, Olivella and Alonso 2008)

$$k_w^{cr} = \frac{b^2}{12}$$



$$k_w = \frac{b^3}{12B}$$

$$b = b_0 + B \langle \varepsilon^n - \varepsilon_0^n \rangle$$

$$k_w = k_{w,0} \left(1 + A \langle \varepsilon^n - \varepsilon_0^n \rangle \right)^3$$

Localised deformation
Fracture initiation

- Empirical law

Related to strain localisation effect
Permeability variation threshold

$$k_{w,ij} = k_{w,ij,0} \left(1 + \beta_{per} \langle YI - YI^{thr} \rangle \hat{\varepsilon}_{eq}^3 \right)$$

$$YI = \frac{II_{\hat{\sigma}}}{II_{\hat{\sigma}}^p}$$

3. Permeability evolution

Modelling of excavation and SDZ experiment

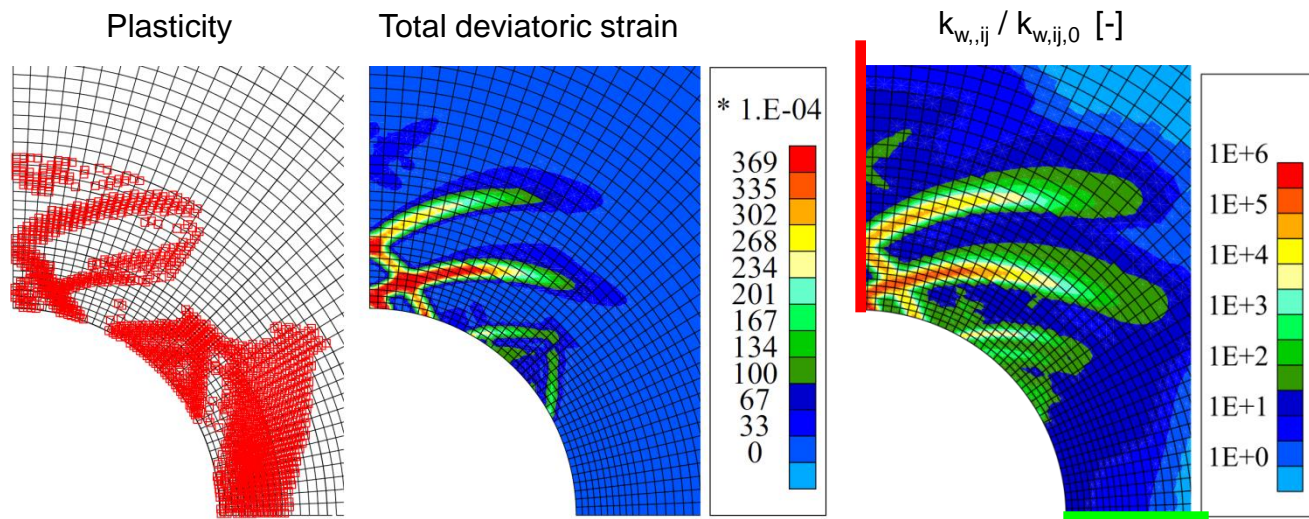
HM coupling in EDZ

- Gallery excavation

SDZ \rightarrow GED gallery // σ_h

Anisotropic $\sigma_{ij,0}$ and material

\rightarrow Localisation zone dominated by stress anisotropy



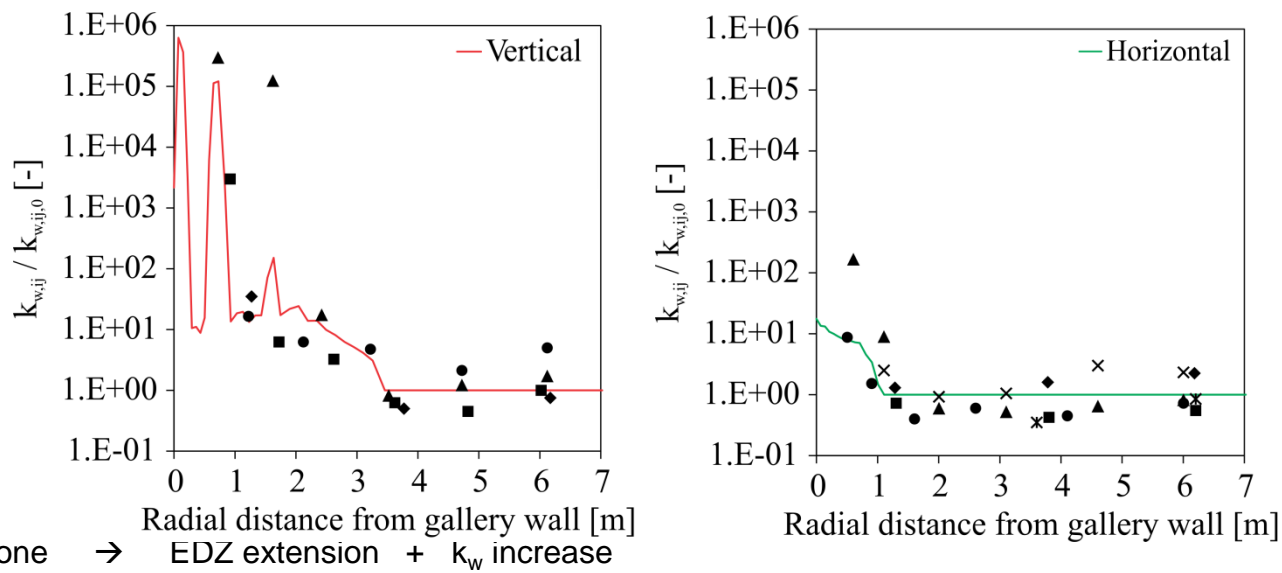
- Intrinsic permeability evolution

$$\frac{k_{w,ij}}{k_{w,ij,0}} = \left(1 + \beta \langle YI - YI^{thr} \rangle \hat{\varepsilon}_{eq}^3\right)$$

$$YI^{thr} = 0.95$$

Cross-sections

Plastic strain and a part of the elastic one



3. Permeability evolution

Modelling of the SDZ experiment

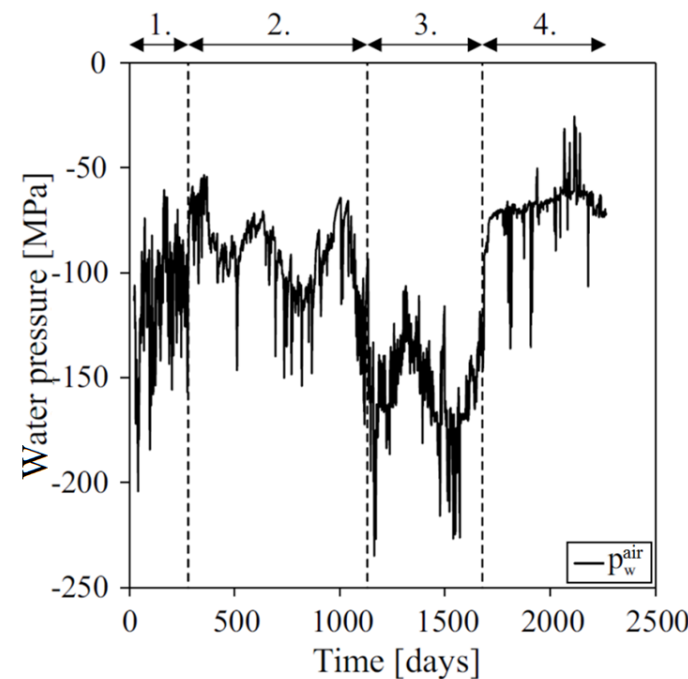
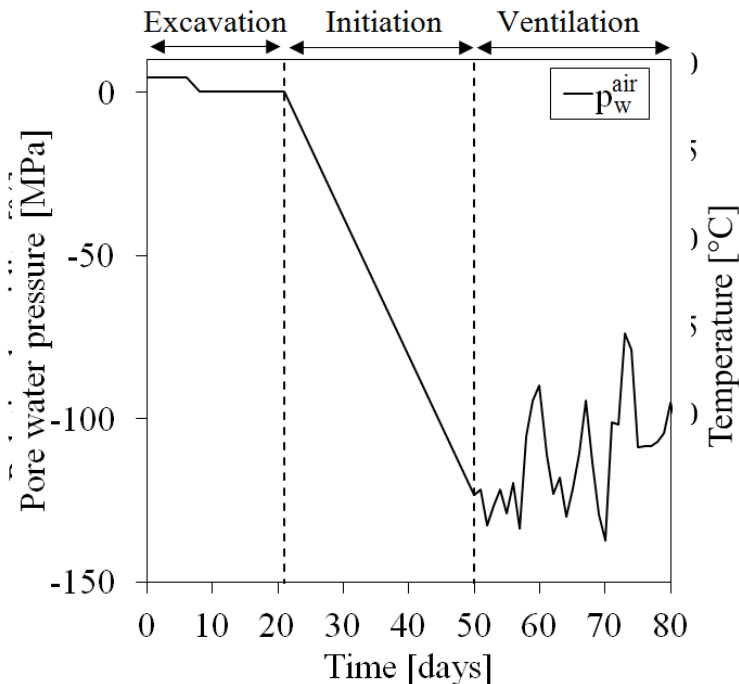
- Water pressure in the cavity air

p_w (suction) corresponding to RH and T (Kelvin's law).

$$p_w^{air} = \frac{\rho_w RT}{M_v} \ln(RH) + p_{atm} \quad \rho_v^{air} = RH \rho_v^0$$

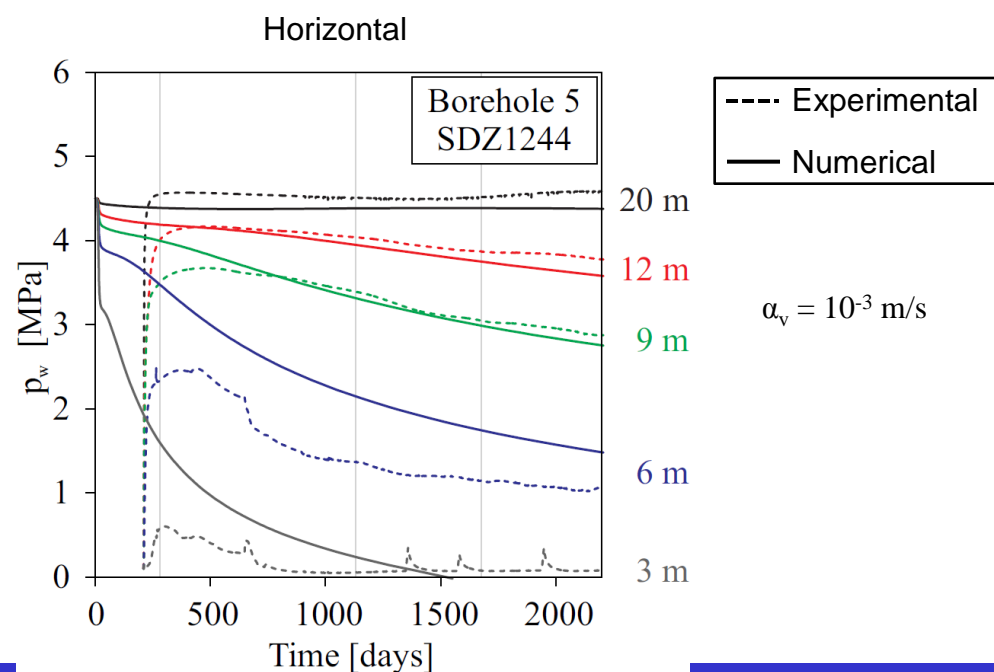
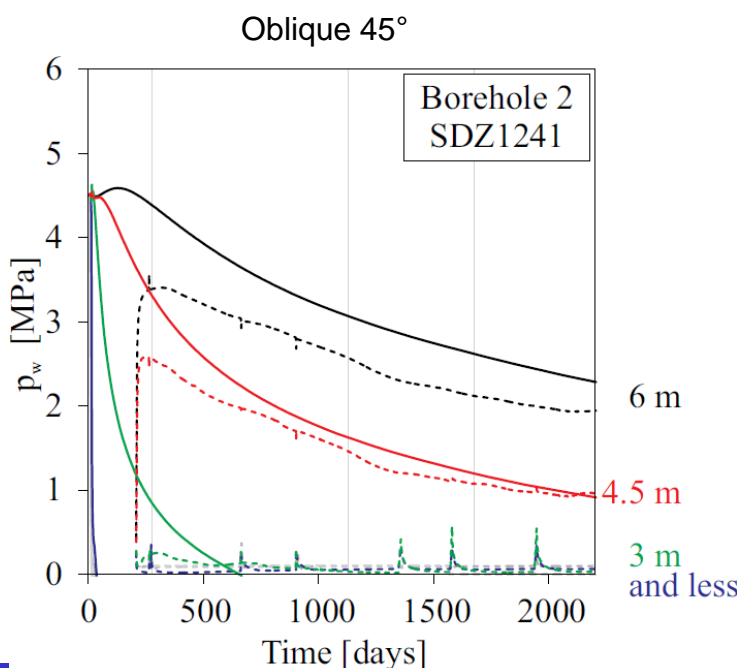
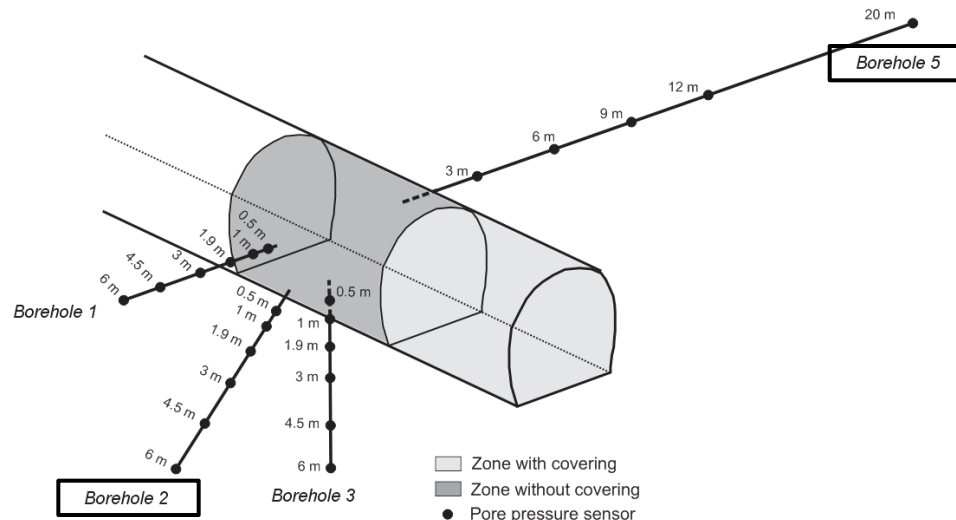
Imposed at gallery wall through hydraulic boundary condition.

Excavation (RH=100%) → Initiation phase → Ventilation



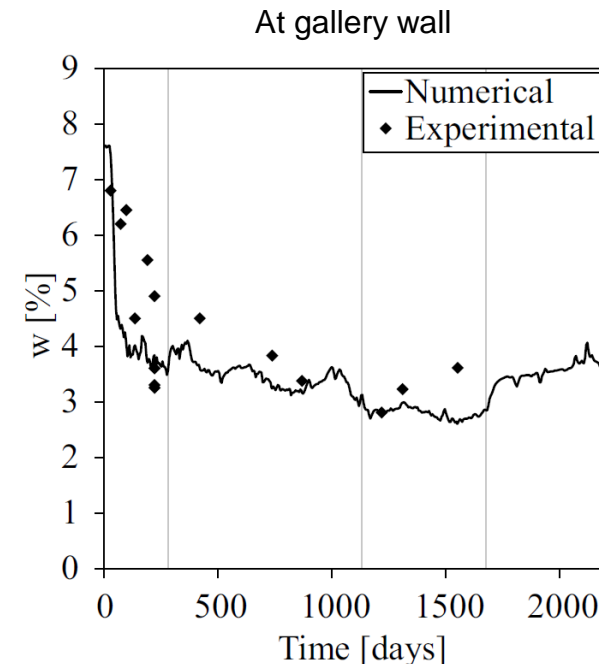
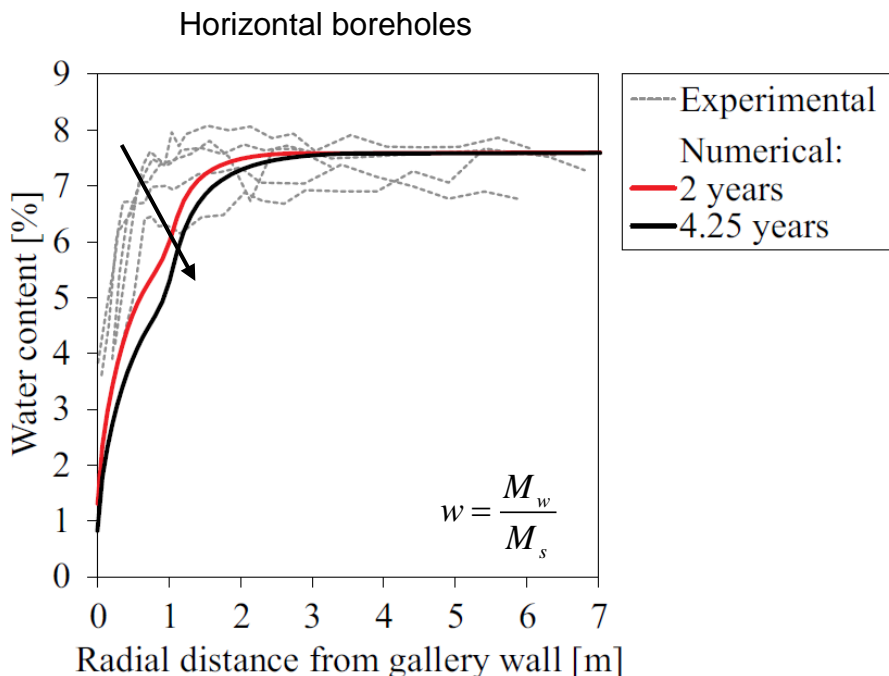
3. Permeability evolution

- Drainage / p_w reproduction



3. Permeability evolution

- Desaturation EDZ / w reproduction



- Desaturation: overestimation in long term
- Vapour transfer ($\alpha_v = 10^{-3} \text{ m/s}$)

→ Good reproduction at gallery wall

Conclusions

- Damaged zone → strain localisation zone similar to *in situ* measurements
- modelling provide information about the rock structure and evolution within this zone, as observed *in situ*.
 - rock anisotropy and properties modification

